




Potential of magnetic quinoa biosorbent composite and HNO₃ treated biosorbent for effective sequestration of chromium (VI) from contaminated water

Sajjad Ahmad, Muhammad Imran, Natasha, Maryam Amin, Abdullah A. Al-Kahtani, Muhammad Arshad, Rab Nawaz, Noor Samad Shah & Ruud J. Schotting


To cite this article: Sajjad Ahmad, Muhammad Imran, Natasha, Maryam Amin, Abdullah A. Al-Kahtani, Muhammad Arshad, Rab Nawaz, Noor Samad Shah & Ruud J. Schotting (2023) Potential of magnetic quinoa biosorbent composite and HNO₃ treated biosorbent for effective sequestration of chromium (VI) from contaminated water, International Journal of Phytoremediation, 25:7, 929-939, DOI: [10.1080/15226514.2022.2122926](https://doi.org/10.1080/15226514.2022.2122926)

To link to this article: <https://doi.org/10.1080/15226514.2022.2122926>

 View supplementary material [↗](#)

 Published online: 19 Sep 2022.

 Submit your article to this journal [↗](#)

 Article views: 99

 View related articles [↗](#)

 View Crossmark data [↗](#)

 Citing articles: 1 View citing articles [↗](#)



Potential of magnetic quinoa biosorbent composite and HNO₃ treated biosorbent for effective sequestration of chromium (VI) from contaminated water

Sajjad Ahmad^a, Muhammad Imran^a, Natasha^a, Maryam Amin^a, Abdullah A. Al-Kahtani^b, Muhammad Arshad^c, Rab Nawaz^d, Noor Samad Shah^a, and Ruud J. Schotting^e

^aDepartment of Environmental Sciences, COMSATS University Islamabad, Vehari, Pakistan; ^bDepartment of Chemistry, College of Science, King Saud University, Riyadh, Saudi Arabia; ^cDepartment of Agriculture and Food Technology, Karakoram International University, Gilgit, Pakistan; ^dDepartment of Environmental Sciences, University of Lahore, Lahore, Pakistan; ^eEnvironmental Hydrogeology Research Group, Department of Earth Sciences, Utrecht University, Utrecht, The Netherlands

ABSTRACT

The present study aims to prepare novel quinoa biosorbent (QB), acid activated QB (QB/Acid) and its nanocomposite with magnetic nanoparticles (QB/MNPs) for batch scale Cr removal from contaminated water. The Cr adsorption was systematically studied at different pH (2–9), adsorbent dosage (1–3 g/L), initial concentration (25–200 mg/L), contact time (180 min) and competing ions in water. Maximum Cr adsorption was observed onto QB/MNPs (57.4 mg/L), followed by QB/Acid (46.35 mg/g) and QB (39.9 mg/g). The Cr removal by QB/MNPs was higher than QB/Acid and QB. Results revealed that the highest Cr removal was obtained at optimum pH 4, 25 mg/L, and 2 g/L dosage. The FTIR spectra displayed various functional groups on adsorbents surface serving as a potential scaffold to remove Cr from contaminated water. The equilibrium and kinetic Cr adsorption data best fitted with Freundlich and pseudo-second order models, respectively ($R^2 \geq 0.96$). The QB/MNPs showed excellent reusability in five adsorption/desorption cycles (4.7% decline) with minor leaching of Fe (below threshold level). The coexisting ions in groundwater showed an inhibitory effect on Cr sequestration (5%) from water. The comparison of Cr adsorption by QB/MNPs and QB/Acid showed better potential for Cr sequestration than various previously explored adsorbents in the literature.

NOVELTY STATEMENT

Quinoa is a cereal crop and after harvesting quinoa straws are either burnt or thrown away which can cause several environmental problems. It would be beneficial to utilize quinoa straws and its modified forms as adsorbents for the water remediation. Therefore, current study aims to estimate the adsorption capacity of quinoa biomass as biosorbent (QB) and its modifications (QB/Acid and QB/MNPs) to treat Cr (VI) contaminated water. The influence of various parameters governing the Cr removal from water has been evaluated. The reusability of QB/MNPs has also been evaluated for its economical use without losing effectiveness for Cr removal from water. The comparison of Cr adsorption by QB/MNPs and QB/Acid showed better adsorption potential for Cr sequestration than various previously explored adsorbents in the literature.

KEYWORDS

Acid activation; chromium; kinetics; magnetic composite; reusability; water contamination

1. Introduction

The quantity and quality of water reservoirs are adversely affected with industrialization, urbanization and modernization (Tariq *et al.* 2020; Kumar A *et al.* 2022). The disposal of industrial effluents into water reservoirs without prior treatment contaminates the surface water and groundwater bodies (Patra *et al.* 2020; Kumar A *et al.* 2022). Water contamination with potentially toxic metals (PTMs) has become a global concern due to their bioaccumulation through food chain (Patra *et al.* 2020; Iqbal MM *et al.* 2021). Chromium (Cr) is one of the PTMs that enters the environment and poses serious threats to environment and human beings due

to its high carcinogenicity, non-degradability, toxicity and mobility (Wang C-C *et al.* 2016; Zhu *et al.* 2017). Water contamination with Cr has become a major concern due to its widespread applications in many industrial activities, *e.g.*, metallurgy, metal processing, textile dyeing, electroplating, wood preservation, chrome based manufacturing, leather tanning, and pigment production (Deng *et al.* 2017; Xie *et al.* 2017; Khalifa *et al.* 2019; Suganya *et al.* 2020). Electroplating utilizes high Cr concentration and releases Cr in effluents up to 2,500 mg/L (Tariq *et al.* 2020). The permissible Cr level in drinking water set by WHO is 0.05 mg/L (Tariq *et al.* 2020). The USEPA has recognized Cr as

priority hazardous pollutant (Lyu *et al.* 2017). Chromium is a redox active metal that mainly occurs in two oxidation states, Cr (III) and Cr (VI), the latter being more noxious to human beings and other living things due to its high aqueous solubility and carcinogenicity (Liu W *et al.* 2014; Din *et al.* 2021). Thus, there is a dire need to treat Cr-contaminated water. The Cr (VI) reduction looks to be an effective approach for its remediation (Liu F *et al.* 2017). For Cr (VI) removal, various approaches like precipitation, reverse osmosis, adsorption, chemical reduction, ion exchange and electro dialysis are employed (Wang H *et al.* 2019; Ou *et al.* 2020; Tariq *et al.* 2020; Din *et al.* 2021). However, due to low efficiency, incomplete removal and high energy consumption these traditional approaches have shortcomings (Gorny *et al.* 2016; Murtaza *et al.* 2019; Iqbal MM *et al.* 2021; Ahmad *et al.* 2022). Adsorption is considered as an active, flexible, and economically practicable alternative in removing Cr from water (Tariq *et al.* 2020; Din *et al.* 2021). Conventional adsorbents such as activated alumina (Mor *et al.* 2007), zeolite (Basaldella *et al.* 2007), chitosan polymer (Hena 2010), activated carbon (Gupta *et al.* 2010), silica gel and bauxite (Shafiq *et al.* 2018) are expensive to remove Cr from contaminated aqueous systems. However, on large scale these adsorbents are not practicable due to complex production, high cost and associated secondary pollution risks. Most of the current research is focused to evaluate the adsorbent potential of easily available, and low cost adsorbent materials (agricultural residues and lignocellulosic waste) for Cr removal *e.g.*, *Eucalyptus camadulensis* seeds (Suganya *et al.* 2020), saw dust, wheat bran (Ogata *et al.* 2020), rice husk (Shamsollahi and Partovinia 2019), citrus peels (Khalifa *et al.* 2019), pea pod, tea, ginger and banana peel (Sharma PK *et al.* 2016), litchi peel (Yi Y *et al.* 2017), water caltrop shell (Kumar S, Narayanasamy, *et al.* 2019). However, some adsorbents are difficult to be reused once pollutants are adsorbed on the adsorbent surface from contaminated water. Moreover, to increase the adsorption potential of the adsorbents different surface modifications are practiced (Naushad *et al.* 2015; Imran *et al.* 2020; Shah NS *et al.* 2020; Tariq *et al.* 2020; Bulgariu *et al.* 2021). Biosorbents are chemically treated to improve the surface functional groups and integrate the counter ions that improve the adsorption potential of various adsorbents (Shah G *et al.* 2019; Imran *et al.* 2020; Suganya *et al.* 2020). Recently, KOH treated corn straw and *Camellia oleifera* seed shell (Guo *et al.* 2018; Ma *et al.* 2019), phosphoric and acid treated apple peels (Enniya *et al.* 2018) are examples of few modified adsorbents effectively utilized for Cr (VI) removal from contaminated aqueous systems. Literature shows that the aggregation and suspension of the adsorbents decrease the adsorption potential of the materials (Suganya *et al.* 2020; Imran *et al.* 2021). To overcome these limitations as well as to improve the surface characteristics (functional groups, particle size and surface area), composites with metallic nanoparticles are considered as the effective modification to treat contaminated water (Tariq *et al.* 2020; Iqbal MM *et al.* 2021; Lucaci *et al.* 2021). Magnetic composites as adsorbents are widely utilized for the treatment of

contaminated water because of its simple preparation and separation after saturation with contaminants (Kumar A *et al.* 2022). In previous studies, ZnO tetrapod and activated carbon composites were utilized for the effective removal of Cr (VI) and it was found that the Cr removal was 97% at pH 2 (Sharma M *et al.* 2019). Zhao *et al.* (2017) utilized magnetic iron oxide/polyacrylonitrile composite for efficient Cr (VI) removal from contaminated water and reported more than 90% Cr removal. Li *et al.* (2016) found that chitosan magnetic composite effectively removed Cr (VI) from contaminated water at pH 2. Li *et al.* (2016) revealed that magnetic particles are rapidly separated and easily regenerated by using simple diluted NaOH solutions and reused with minor decline in adsorption capacity.

The current study aims to evaluate the adsorption capacity of quinoa biomass as biosorbent (QB) and its modifications (QB/Acid and QB/MNPs) to treat Cr (VI) contaminated water. Quinoa is a cereal crops and is considered a good replacement for the commercially cultivated grain crops owing to its higher nutritional value (Jarvis *et al.* 2017; Shabbir *et al.* 2021). Quinoa is identified as a climate resilient crop against abiotic stress, and it gives higher yield even on marginal lands with low economic input requirements (Ruiz *et al.* 2016). Quinoa straws after harvesting are either burnt or thrown away which leads to several environmental problems (Imran *et al.* 2020; Naeem *et al.* 2020). Hence, it would be beneficial to utilize quinoa straws and its modified forms as adsorbents for water remediation. The influence of various parameters governing the Cr removal from water has also been evaluated. The equilibrium and kinetic adsorption data have been simulated with equilibrium and kinetic adsorption isotherm models. The impact of coexisting ions in water and reusability of QB/MNPs has also been estimated for Cr sequestration from contaminated water. Moreover, the adsorption potential of QB, QB/Acid and QB/MNPs for Cr removal was compared with the previously used adsorbents in the literature.

2. Material and methods

2.1. Chemicals and reagents

Hydrochloric acid (HCl), nitric acid (HNO₃), sodium hydroxide (NaOH), ferric chloride (FeCl₃), Ferrous sulfate (FeSO₄), potassium dichromate (K₂Cr₂O₇) and potassium hydroxide (KOH) were used in the batch scale experiments. A 0.1M NaOH and HCl solutions were utilized to adjust the solution pH during experimentation. A stock solution of Cr (500 mg/L) was prepared with K₂Cr₂O₇ salt in distilled water (DW). Further solutions of various Cr concentrations were prepared with dilution method. The chemicals were of analytical grade purchased from Merk, Faisalabad and were used without further purification.

2.2. Preparation of QB and its surface modification

For the preparation of quinoa biosorbent (QB), dry biomass of quinoa was collected locally from the field after

harvesting. The quinoa biomass was washed with DW thoroughly to get rid of the adhered dirt and unwanted constituents. The air-dried biomass was oven dried for 36 h at 60 °C. The oven-dried biomass of quinoa was pulverized to fine powder and preserved for further applications.

To prepare the QB composite with acid (QB/Acid), 25 g QB was immersed in 200 ml HNO₃ solution (5%) with vigorous mixing of the constituents. The mixture was kept on a shaker for 1 h and then filtered using Whatman filter paper. The acid modified QB was washed with DW and again filtered to purify the QB/Acid. The resultant QB/Acid was air dried and kept in the oven at 65 °C. While magnetic composite of QB (QB/MNPs) was prepared with precipitation method (Imran *et al.* 2019; Iqbal MM *et al.* 2019; Iqbal MM *et al.* 2021). A 10% solution of FeSO₄ (w/v) and 10% solution of FeCl₃ (w/v) was prepared in DW. Subsequently, a homogeneous mixture of FeSO₄ and FeCl₃ was prepared by taking 4 mL of FeCl₃ and 8 mL of FeSO₄ in 250 mL beaker and 0.5 g of QB was added and thoroughly mixed. The resultant mixture was titrated against 0.15 M KOH dropwise to prepare the composite QB/MNPs. Subsequently, the solution was filtered, oven dried and pulverized to fine material. The prepared QB, QB/Acid and QB/MNPs were preserved in separate containers for the experiments and characterization.

2.3. FTIR analysis and measurement of point of zero charge

It is crucial to determine the functional groups of the prepared QB, QB/Acid and QB/MNPs to understand and justify the adsorption mechanism for the treatment of contaminated systems (Murtaza *et al.* 2019; Shah NS *et al.* 2020; Imran *et al.* 2021). The QB, QB/Acid and QB/MNPs used in the current study were characterized with FTIR (Thermo Scientific Nicolet-6700TM, USA) to find the functional groups on their surface. The FTIR spectra of pristine and Cr-loaded QB, QB/Acid and QB/MNPs were achieved in 600–4,000 cm⁻¹. The QB, QB/Acid and QB/MNPs adsorbents were also characterized by measuring their point of zero charge (PZC) because it is considered as a pH at which the adsorbent is neutral or exhibits zero charge on the surface after the adsorbent interaction with the electrolyte. The PZC of QB, QB/Acid and QB/MNPs adsorbents was estimated by following Imran *et al.* (2019) and Tariq *et al.* (2020).

2.4. Batch scale adsorption studies

The batch scale adsorption/removal experiments were performed in 250 mL Erlenmeyer flasks at ambient temperature (25 ± 2 °C). The effect of different factors *i.e.*, pH (2, 4, 6 and 9), adsorbent dose (1, 2 and 3 g/L), initial concentration (25–200 mg/L) and time (15–180 min) was evaluated on Cr (VI) adsorption onto QB, QB/Acid and QB/MNPs. The Cr containing water was agitated on a mechanical shaker for 3 h at 150 rpm. The residual level of Cr was measured in water samples taken after 15, 30, 60, 120 and 180 min. The

Table 1. Concentration of cations and anions, EC (dS/m, TDS (mg/L) and Cr (mg/L) in the groundwater samples (GW1 and GW2) to assess the influence of coexisting ions on Cr removal.

Parameter	Unit	GW 1	GW 2
EC	dS/m	1.93	1.12
pH	–	8.0	7.5
TDS	mg/L	985	650
CO ₃ ²⁻	mg/L	160	76
HCO ₃ ⁻	mg/L	640	312
Cl ⁻	mg/L	850	465
SO ₄ ²⁻	mg/L	510	315
NO ₃ ⁻	mg/L	32.5	22.1
Na ⁺	mg/L	260.5	145
K ⁺	mg/L	7.6	5.8
Ca ²⁺	mg/L	85.6	55.0
Cr	mg/L	0.011	0.025

Cr removal from contaminated water was optimized for the adsorbent dosage, solution pH and interaction time. The impact of competing ions in water on Cr removal was evaluated by conducting experiment with two groundwater samples (GW 1 and GW2) having characteristics given in Table 1. The GW1 and GW2 were investigated for pH, electrical conductivity (EC), total dissolved solids (TDS), Nitrate (NO₃⁻), sulfate (SO₄²⁻), chloride (Cl⁻), Carbonates (CO₃²⁻) and bicarbonates (HCO₃⁻), sodium (Na⁺), calcium (Ca²⁺) and potassium (K⁺). The concentration of Na⁺, K⁺ and Ca²⁺ was determined with Flame photometer. The EC (dS/m), TDS (mg/L) and pH were measured with a multiparameter meter (3 in one) Hanna meter (HI98129). The concentration (mg/L) of NO₃⁻, and SO₄²⁻ was measured with UV/Vis spectrophotometer (Perkin-Elmer Lambda 25, Germany). The CO₃²⁻, HCO₃⁻ and Cl⁻ concentrations (mg/L) in groundwater were measured with titration method (Estefan 2013). Moreover, water samples were analyzed for Cr content via Atomic Absorption Spectrometer (PerkinElmer Atomic Absorption Spectrometer). The Cr removal (%) by QB, QB/Acid and QB/MNPs was calculated using Eq. (1) (Imran *et al.* 2019; Shah *et al.* 2022). The ability of the QB, QB/Acid and QB/MNPs to adsorb Cr on the respective surface was calculated with Eq. (2) (Din *et al.* 2019; Murtaza *et al.* 2019).

$$R(\%) = \left(\frac{C_0 - C_f}{C_0} \right) \times 100 \quad (1)$$

$$q_e(\text{mg/g}) = \left(\frac{C_0 - C_f}{M_b} \right) \times V \quad (2)$$

In Eqs. (1) and (2), C₀ and C_f represents the initial and final Cr levels in water after interaction with the adsorbents (mg/L). In Eq. (2), q_e represents Cr (mg) adsorbed per mass (g) of the adsorbent, M_b is the adsorbent mass (g) used for the interaction and V represents the volume of Cr contaminated solution (L). To calculate kinetic Cr adsorption q_t at time t onto QB, QB/Acid, QB/MNPs surface, C_f in Eq. (2) was substituted with Cr concentration C_t at time t.

2.5. Modeling isotherm equilibrium and kinetic adsorption

The experimental Cr (VI) adsorption onto QB, QB/Acid and QB/MNPs was validated with Freundlich, Langmuir, Temkin and Dubinin-Radushkevich (DR) adsorption isotherm models. Freundlich model (Eq. (3)) was applied to examine the multilayer adsorption mechanism that occurs on nonuniform surfaces with intermolecular interactions between the adsorbed ions on adjacent active sites (Akram *et al.* 2019; Hussain *et al.* 2020; Sharma G and Naushad 2020).

$$q_e = K_F C_e^{1/n} \quad (3)$$

where K_F in Eq. (3) is Freundlich model constant, q_e is model adsorption at equilibrium and $\frac{1}{n}$ indicates adsorbent heterogeneity on its surface. Linear form of Freundlich model (Eq. (4)) was employed to determine the model parameters from the intercept (K_F) and slope ($\frac{1}{n}$) of the respective curve between $\ln(q_e)$ versus $\ln(C_e)$ (Vigneshwaran *et al.* 2021).

$$\ln(q_e) = \left[\ln(K_F) + \left(\frac{1}{n}\right) \ln(C_e) \right] \quad (4)$$

Langmuir model (Eq. (5)) was applied to examine the monolayer Cr adsorption on finite number of adsorption sites onto QB, QB/Acid and QB/MNPs surface (Vilela *et al.* 2019; Din *et al.* 2021).

$$q_e = \left(\frac{K_L C_e q_{max}}{1 + K_L C_e} \right) \quad (5)$$

In Eq. (5), q_e is adsorption capacity of adsorbents (QB, QB/Acid and QB/MNPs) at equilibrium, C_e is equilibrium concentration, K_L is Langmuir constant and q_{max} is the maximum Cr adsorption at equilibrium. The linear form of Langmuir model (Eq. (6)) was used to estimate Langmuir model parameters (Ahmad *et al.* 2017; Imran *et al.* 2020) from the slope ($\frac{1}{q_{max}}$) and intercept ($\frac{1}{K_L q_{max}}$) of the respective curve for Cr adsorption on QB, QB/Acid and QB/MNPs.

$$\frac{C_e}{q_e} = \left(\frac{1}{K_L q_{max}} + \frac{C_e}{q_{max}} \right) \quad (6)$$

$$q_e = B \ln A + B \ln C_e \quad \text{where} \quad B = \frac{RT}{b} \quad (7)$$

$$\ln q_e = \ln q_m - k_{DR} \varepsilon^2 \quad \text{where} \quad \varepsilon = \left[RT \ln \left(1 + \frac{1}{C_e} \right) \right] \quad (8)$$

In Temkin model (Eq. (7)), b (J/g/mol) and K_T (kJ/mol) indicate equilibrium-binding-constants in Temkin model, T (K) is the temperature and R is universal gas constant. The values of Temkin model parameters (b and K_T) were estimated from the slope ($\frac{RT}{b}$) and intercept ($\frac{RT}{b} K_T$) of the curve between q_e and $\ln(C_e)$. Moreover, according to linear form of DR model (Eq. (8)), a graph between $\ln(q_e)$ versus ε^2 was plotted to calculate the values of DR model parameters (q_m , k_{DR}) from the respective slope and

intercept of the curves for Cr adsorption onto QB, QB/Acid and QB/MNPs.

The kinetic experimental Cr (VI) adsorption onto QB, QB/Acid and QB/MNPs (at 50 mg Cr/L) was simulated with pseudo 1st order (Eq. (9)), pseudo 2nd order (Eq. (10)) and intra-particle diffusion (Eq. (11)) models.

$$\log(q_e - q_t) = \left[\log(q_e) - \left(\frac{k_1}{2.303} \right) \times t \right] \quad (9)$$

$$\frac{t}{q_t} = \frac{1}{k_2 (q_e)^2} + \frac{t}{q_e} \quad (10)$$

$$q_t = k_d t^{0.5} + C \quad (11)$$

Where q_t is Cr adsorption at time (t), q_e is Cr adsorption at equilibrium and k_1 is pseudo 1st order rate constant. A graph was drawn between t versus $\log(q_e - q_t)$, to find the values of first order model parameters from the intercept ($\log(q_e)$) and slope ($\frac{k_1}{2.303}$) of the respective curve.

In Eq. (10), k_2 is pseudo 2nd order rate constant. A graph was drawn between t versus $\frac{t}{q_e}$ to estimate the pseudo 2nd order model parameters from the intercept ($\frac{1}{k_2 (q_e)^2}$) and slope ($\frac{1}{q_e}$) of the curve. Moreover, in Eq. (11), k_d is the diffusion model constant and C is the boundary layer thickness (Din *et al.* 2021). The values of intra-particle diffusion model parameters were estimated from the slope and intercept of the curve for Cr adsorption onto QB, QB/Acid and QB/MNPs.

2.6. Reusability and stability of QB/MNPs

It is crucial to determine the adsorbents reusability and stability for removing certain contaminant from the contaminated water. Therefore, based on the maximum Cr adsorption potential of QB/MNPs, only QB/MNPs was tested for the reusability in five adsorption and desorption cycles at 50 mg Cr/L, pH-4, dose 2 g/L and equilibrium. The QB/MNPs with attached Cr were recovered by rinsing it with HCl (4%) solution followed with DW washing after each adsorption cycle. The rinsed QB/MNPs were filtered and oven-dried to reuse it for Cr sequestration from contaminated water. The residual Cr concentration after each adsorption cycle was measured to evaluate its reusability potential and was compared with the first cycle. The QB/MNPs stability was evaluated by measuring the Fe concentration leached during acid washing of Cr containing QB/MNPs (Hussain *et al.* 2020; Iqbal MM *et al.* 2021).

3. Results and discussion

3.1. Ftir analysis and point of zero charge measurement

The FTIR analysis was carried out to find the functional groups involved in Cr (VI) removal onto the surface of QB and its modified forms (QB/Acid, QB/MNPs) (Figure 1). The spectral range for FTIR analysis was taken from 600–4,000 cm^{-1} for the Cr (VI) removal by QB, QB/Acid,

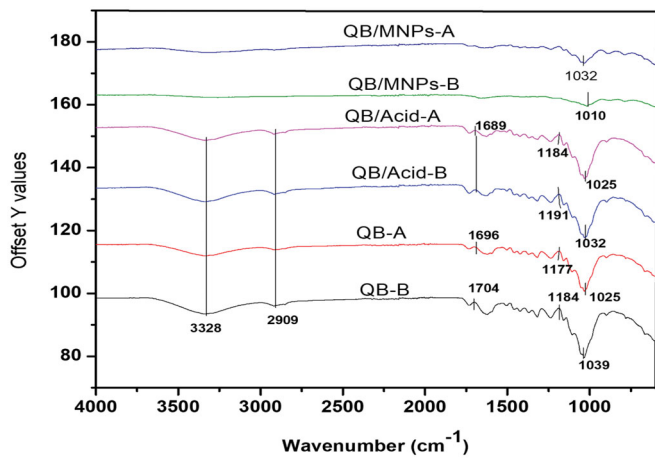


Figure 1. FTIR analysis of QB, QB/Acid and QB/MNPs before (B) and after (A) Cr adsorption.

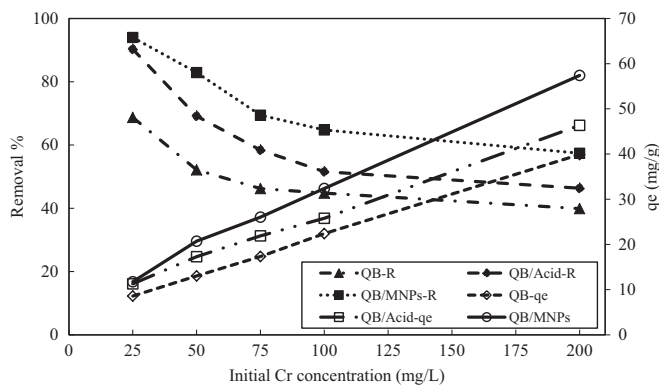


Figure 2. Effect of initial Cr level on its removal and adsorption onto QB, QB/Acid and QB/MNPs at dose 2 g/L, pH-4 and equilibrium.

and QB/MNPs. The broad peaks at $3,328\text{ cm}^{-1}$ matches with O-H alcoholic functional group and $2,909\text{ cm}^{-1}$ indicates alkane groups (C-H) (Khan *et al.* 2021). The transmission at $1,704$, $1,689$ and $1,696\text{ cm}^{-1}$ corresponds to weak stretching due to alkenes (C=C) (Patra *et al.* 2020). Clear transmission bands were visible at $1,010$ – $1,104$, $1,175$ – $1,190$, $2,909$ and $3,328\text{ cm}^{-1}$. The FTIR spectra showed that QB/MNPs did not possess OH and C-H groups. Absorbance at $1,010$ – $1,190\text{ cm}^{-1}$ indicates C-O and C-N (Khan *et al.* 2019; Imran *et al.* 2021). The FTIR spectra revealed a change in the transmission bands depending on the Cr loading and nature of the adsorbent. The Cr-loaded adsorbents demonstrated more absorbance on the adsorbent surface. In the functional group region, all the adsorbents showed peaks almost at the same wavenumber, but the absorbance varies for Cr-loaded and unloaded materials. The absorbance was maximum for QB/MNPs as compared with QB/Acid and QB either in the presence or absence of Cr.

The PZC values for QB, QB/MNPs and QB/Acid were 7.1, 6.1 and 5.4, respectively. Literature shows that for anionic pollutants (e.g., Cr as chromate), contaminant adsorption is high if aqueous solution has $\text{pH} < \text{PZC}$. It is possibly due to the protonation of the adsorbent surface (H^+) at low pH (Imran *et al.* 2019; Naeem *et al.* 2019; Imran *et al.* 2020). This difference in functional groups and

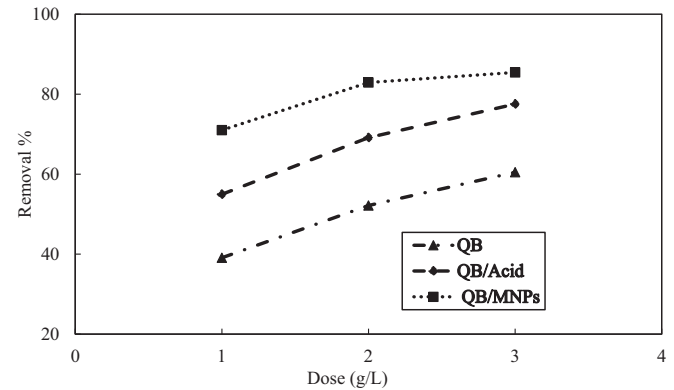
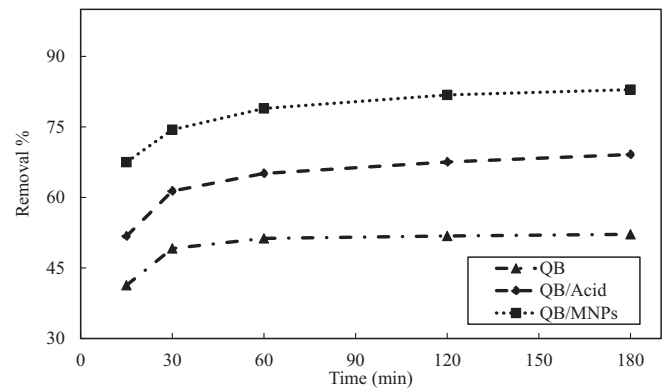


Figure 3. (a) Effect of contact time on chromium removal by QB, QB/Acid and QB/MNPs at 2 g/L material dose, pH-4 and 50 mg Cr/L, (b) Effect of dose of QB, QB/Acid and QB/MNPs on chromium removal at 50 mg Cr/L, pH-4 and equilibrium.

PZC of QB, QB/Acid and QB/MNPs is responsible for their different potential to remove Cr from contaminated water.

3.2. Effect of initial Cr concentration

The initial Cr concentration plays a key role for its sequestration by an adsorbent at a fixed dose. Figure 2 demonstrated the effect of initial Cr concentration (25–200 mg/L) on the removal and adsorption of Cr by QB, QB/Acid, and QB/MNPs. The results depicted that the Cr removal decreased by 69–40%, 90–46%, and 97–57% correspondingly for QB, QB/Acid, and QB/MNPs when Cr concentration increased from 25 to 200 mg/L. The highest Cr removal (97%) was attained by QB/MNPs at lower concentration (25 mg Cr/L). High Cr concentration linearly increased adsorption capacities of the adsorbents while decreased Cr removal from contaminated aqueous system. There is a quick increase in Cr adsorption at initial stage because of great interaction of Cr molecules with the adsorption sites and electrostatic attraction which resulted into gradual increase in Cr adsorption at higher concentration. The Cr adsorbed by QB, QB/Acid and QB/MNPs was 39.9, 46.35 and 57.4 mg/g, respectively. Higher Cr concentration acts as a governing force to reduce the resistance of mass transfer of Cr molecules among solid and liquid phase (Kumar A, Thakur, *et al.* 2019; Tariq *et al.* 2020). Moreover, aggregation of the adsorbent particles and incomplete occupation of sites are the crucial aspects affecting the removal of Cr (Aigbe *et al.* 2018; Din *et al.* 2021). The high metal

concentration favors the formation of oxide/hydroxide (Aigbe and Osibote 2020) and improves Cr adsorption at its elevated concentrations.

3.3. Effect of contact time

Figure 3a presents the impact of contact time (15–180 min) on Cr removal by QB, QB/Acid, and QB/MNPs at constant adsorbents dose (2 g/L), initial concentration (50 mg Cr/L) and pH-4. The results disclosed that Cr removal increased by 41–52%, 52–69%, and 68–83% respectively by QB, QB/Acid, and QB/MNPs when the contact time increased from 15–180 min. The maximum removal was obtained in first 30 mins and then a minor increase was observed with increasing contact time which became steady to attain equilibrium (Figure 3a). It might be credited to high surface area and availability of more adsorption places during first 30 min that can readily uptake Cr ions (Tariq *et al.* 2020). With time, the repulsive forces became dominant between the solid and liquid phase and there is decline in the removal rate (Pradhan *et al.* 2019; Din *et al.* 2021). Overall, results revealed that maximum Cr removal with QB, QB/Acid and QB/MNPs adsorbents used in the current study was achieved in first 30 min of interaction between the adsorbents and Cr in simulated contaminated water.

3.4. Effect of adsorbent dose

The optimization of material dosage in adsorption experiment is a central parameter that controls the capacity of an adsorbent for the efficient removal of contaminants from aqueous systems (Imran *et al.* 2020; Iqbal MM *et al.* 2021). Figure 3b represents the effect of QB, QB/Acid and QB/MNPs dosage (1–3 g/L) on Cr removal at 50 mg Cr/L, pH-4 and equilibrium. The results revealed an increasing trend in Cr removal with an increase in QB, QB/Acid and QB/MNPs dosage. The increase in Cr removal was: 39–60%, 55–78%, and 71–85%, respectively for QB, QB/Acid, and QB/MNPs when dose was varied from 1–3 g/L. This increase in Cr removal with dose is attributed to the availability of the more active sites for Cr adsorption at higher dose (Shakya and Agarwal 2019; Hussain *et al.* 2020). At lower adsorbent dosage, there exists a competition between Cr ions to occupy the available sites (Tariq *et al.* 2020). However, at higher adsorbent dosage, there are plenty of active sites available for the Cr and competition decreases leading to higher removal efficiency at elevated dose of each adsorbent (Aljerf 2018). The difference in Cr removal (%) was higher when the adsorbent dosage was changed from 1–2 g/L as compared with Cr removal when adsorbent dosage changed from 2–3 g/L due to occupation of more active sites and decline in active surface area of sorbent per unit mass. Therefore, the optimum dose considered for the Cr adsorption onto QB, QB/Acid and QB/MNPs was 2.0 g/L. The highest Cr removal of 85% was observed by QB/MNPs at 2 g/L. The increase in Cr removal by QB/MNPs is attributed to the improvement in its total surface area, surface characteristics and the availability of active exchangeable sites for the attachment of Cr ions. There is decline in Cr

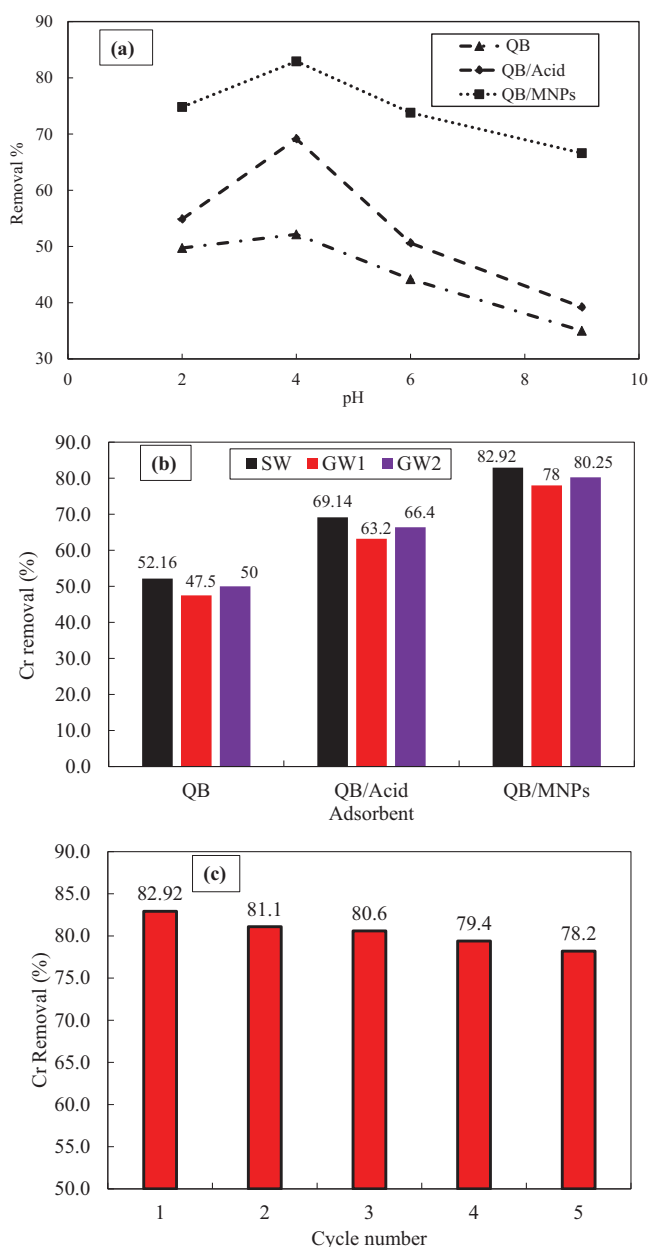


Figure 4. (a) Effect of pH on chromium removal with QB, QB/Acid and QB/MNPs at Cr concentration of 50 mg/L, 2 g/L material dose and equilibrium; (b) impact of inorganic ions on Cr removal when Cr level (50 mg/L) was developed in two groundwater samples (GW1 and GW2) having different concentrations of ions; (c) reusability of QB/MNPs.

adsorption at higher dose (data not presented) due to limited availability of Cr ions to occupy the adsorption sites at higher dosage of the adsorbent (Patra *et al.* 2020).

3.5. Effect of solution pH

The pH of aqueous Cr (VI) solution plays a vital role in its sequestration by the adsorbents due to surface protonation and deprotonation. Figure 4a shows the influence of solution pH (2–9) on Cr removal by QB, QB/Acid, and QB/MNPs keeping other parameters constant *i.e.*, Cr concentration (50 mg/L), time (180 mins) and dose (2 g/L). Results show that the Cr removal increased when pH was raised from 2

Table 2. Parameters of equilibrium adsorption (Langmuir, Freundlich, Temkin and Dubinin-Radushkevich) and kinetic adsorption (Pseudo 1st order, Pseudo 2nd order, and intra-particle diffusion) models.

Type	Model	Parameter	QB	QB/Acid	QB/MNPs
Equilibrium adsorption models	Langmuir	K_L (L/mg)	0.012	0.031	0.045
		q_{max} (mg/g)	54.64	62.11	66.67
		R^2 (-)	0.77	0.82	0.85
	Freundlich	K_F ((mg/g(L/mg) ^{1/n}))	2.45	7.41	6.30
		n (-)	1.79	2.88	2.71
		R^2 (-)	0.96	0.95	0.96
	Temkin	K_T (L/g)	1.68	0.08	0.23
		b (J/g/mol)	229.33	308	249.92
		R^2 (-)	0.83	0.75	0.80
	Dubinin-Radushkevich	q_m (mg/g)	22.53	26.28	21.52
		k_{DR} (kJ/mol)	11.33	1.16	0.53
		R^2 (-)	0.57	0.53	0.61
Kinetic adsorption models	Pseudo-first order	k_1 (1/min)	0.069	0.049	0.013
		q_e (mg/g)	2.39	2.45	4.50
		R^2 (-)	0.87	0.94	0.86
	Pseudo-second order	k_2 (g/mg/min)	0.025	0.010	0.011
		q_e (mg/g)	13.28	17.76	21.19
		R^2 (-)	0.999	0.99	0.99
	Intra-particle diffusion	k_d	0.23	0.39	0.37
		C	10.39	12.46	16.18
		R^2 (-)	0.62	0.80	0.86

to 4. However, Cr removal diminished by 83–67%, 69–39% and 52–35% with QB/MNPs, QB/Acid, and QB, respectively, when pH varied from 4 to 9 which confirmed a clear dependence of Cr removal on the system pH. Chromium removal was maximum at pH 4 because the surface of adsorbents was positively charged at this pH and HCrO_4^- ions showed more electrostatic pull toward adsorbents surface due to protonation (Aigbe and Osibote 2020; Tariq *et al.* 2020, Din *et al.* 2021). In acidic media, the adsorbent surface is highly protonated (excess H^+ presence) (Huang *et al.* 2020). Hence, great electrostatic attraction occurs between the positively charged surface and anionic Cr as CrO_4^{2-} , thereby facilitating the adsorption at low pH (Yi G *et al.* 2017; Aigbe and Osibote 2020). Contrarily, higher pH with more OH ions showed reduction in Cr adsorption and its removal (Ali A *et al.* 2016; Tariq *et al.* 2020) due to deprotonation of the adsorbent surface. Noticeably, highest Cr removal (83%) was achieved by QB/MNPs as compared to QB/Acid, and QB due to dual properties of biosorbent and MNPs. This high Cr adsorption onto QB, QB/Acid and QB/MNPs is also justified from PZC because adsorption of an anionic contaminant is favored by the adsorbents at $\text{pH} < \text{PZC}$ (Imran *et al.* 2019; 2021; Iqbal MM *et al.* 2021).

3.6. Impact of coexisting ions in water

The natural groundwater contains various cations and anions, and their coexistence greatly affects the adsorption of aqueous Cr (chromate) onto the adsorbent surface (Maitlo *et al.* 2019; Zeng *et al.* 2021). In the current study, the impact of coexisting anions (NO_3^- , SO_4^{2-} , Cl^- , CO_3^{2-} and HCO_3^-) and cations (Na^+ , K^+ , Ca^{2+}) on Cr removal by QB, QB/Acid and QB/MNPs was evaluated by using two groundwater samples (GW1 and GW2). The concentration of different cations and anions in GW1 and GW2 is given in Table 1. Figure 4b displays the impact of coexisting ions on Cr removal at optimum pH 4, dose 2 g/L and 50 mg/L initial Cr concentration under equilibrium. The inherent Cr

concentration in GW1 and GW2 was 0.011 and 0.025 mg/L, respectively. The maximum decline in Cr removal with QB in GW1 and GW2 was 4.66% and 2.16% and while with QB/Acid respective decline in Cr removal was 5.96% and 2.7% as compared with synthetic water (SW). But decline in Cr removal with QB/MNPs in GW1 and GW2 was 4.9 and 2.67% as compared with SW. The results (Figure 4b) revealed a more decline in Cr removal by GW1 onto QB, QB/Acid and QB/MNPs as compared with GW2 which is accredited to higher concentration of anions in GW1 than GW2. Maitlo *et al.* (2018) evaluated the impact of different concentrations of interfering ions on the efficiency of adsorbents for the treatment of Cr contaminated water. They found that the presence of PO_4 in water significantly hindered the Cr adsorption onto iron hydroxides as compared with silicate and other ions present in natural water. The results of the present study are in line with the previous finding that the presence of competing anions in water inhibited the Cr (VI) removal (Su *et al.* 2019; Zeng *et al.* 2021).

3.7. Reusability and stability of QB/MNPs

The stability and reusability potential of QB/MNPs for the Cr adsorption was evaluated due to maximum Cr adsorption onto QB/MNPs as compared with QB and QB/Acid. Figure 4c presents the results for Cr removal when QB/MNPs was evaluated for its reusability in five adsorption/desorption cycles at Cr concentration of 50 mg/L under optimum dose and pH. The results revealed a 4.7% decline in Cr removal after five adsorption/desorption cycles which indicates cost effective reuse of QB/MNPs composite for Cr sequestration from aqueous system. There was 1.0, 1.82, 2.32, 3.52 and 4.7% decline in Cr removal in 1st, 2nd, 3rd, 4th and 5th desorption cycle. Likewise, Fe concentration leached from QB/MNPs during its recovery in 1st, 2nd, 3rd, 4th and 5th desorption cycle was 0.05, 0.07, 0.08, 0.11 and 0.13 mg/L which are lower than the permissible level of Fe

Table 3. Comparison of adsorption/removal potential of the adsorbents used in the present study with the previously explored adsorbents in the literature.

Materials	Adsorption (mg/g)	Reference
Quinoa biosorbent	39.9	This study
Quinoa biosorbent/acid activated	46.35	This study
Quinoa biosorbent/magnetic nanoparticles composites	57.4	This study
Calcite based biocomposite	49	(Mishra <i>et al.</i> 2020)
Algal bloom/Iron-carbon composites	43	(Cui <i>et al.</i> 2019)
Chitosan carbonized rice husk	55.4	(Sugashini and Begum 2013)
Artemisia monosperma/trimethyloctadecylammonium bromide	36.9	(Ali HM <i>et al.</i> 2021)
Lantana camara/acid treated	362.8	(Nithya <i>et al.</i> 2020)
Food materials/citric acid	11.5	(Zhang <i>et al.</i> 2020)
Activated carbon/micro-sized goethite	27.2	(Su <i>et al.</i> 2019)
Acid modified biomass	163.51	(Patra <i>et al.</i> 2019)

in water as per WHO limits. It is concluded from the reusability and stability results that QB/MNPs can be well reused upto certain number of adsorption/desorption cycles for the Cr removal from water without losing its effectiveness.

3.8. Modeling of equilibrium and kinetic adsorption

Freundlich, Langmuir, Temkin and DR isotherm models were employed for the simulation of equilibrium adsorption experiments. The value of regression coefficient (R^2) was chosen to determine the suitability of model. The correlation behavior of equilibrium adsorption models for Cr adsorption onto QB, QB/Acid and QB/MNPs has been presented in SS Figure 1. The values of model parameters including R^2 have been provided in Table 2. The simulation results show change in the values of models parameters for Cr adsorption with the adsorbent type which indicates variation in surface characteristics of QB, QB/Acid and QB/MNPs to adsorb Cr from contaminated aqueous system. For Langmuir isotherm model, the q_{max} values for QB, QB/Acid and QB/MNPs were 54.64, 62.11 and 66.67 mg/g, respectively. The respective K_L values for QB, QB/Acid and QB/MNPs were 0.012, 0.031 and 0.045. The R^2 value was higher for QB/MNPs (0.85) than QB and QB/Acid. For Freundlich isotherm model, the n value was higher for QB/Acid (2.88) as compared with n values for QB/MNPs and QB. The comparison of DR, Temkin, Freundlich and Langmuir models for Cr adsorption shows that Freundlich model well explained the Cr adsorption onto QB, QB/Acid and QB/MNPs ($R^2 \geq 0.95$).

To evaluate the kinetics of Cr adsorption onto QB, QB/Acid and QB/MNPs, pseudo-first order, pseudo-second order and intra-particle diffusion models were employed. The values of kinetic models' parameters including R^2 are presented in Table 2 while models fitting behavior with experimental data have been shown in SS Figure 2. The simulation results for Cr adsorption indicated decreasing trend in k_1 onto QB, QB/Acid and QB/MNPs. Similarly, the values of k_2 were 0.25, 0.1 and 0.11, respectively for QB, QB/Acid and QB/MNPs. The maximum k_d value (0.39) of intra-particle diffusion model was obtained with QB/Acid. The comparison of kinetic models' response for Cr adsorption based on the value of R^2 revealed that the kinetic experimental adsorption data with all the three adsorbents (QB, QB/Acid and QB/MNPs) was well explained with pseudo-second order model ($R^2 = 0.99$). The trend of models' suitability for kinetic adsorption of Cr was

pseudo-second order > pseudo-first order > intra-particle diffusion. Similar response for kinetic adsorption of Cr with pseudo-second order was obtained by Tariq *et al.* (2020) and Din *et al.* (2021).

3.9. Comparison of adsorption potential with literature

The Cr adsorption potential onto QB, QB/Acid and QB/MNPs nanocomposite from contaminated water has been compared with various other previously explored adsorbents (Table 3). The comparison with literature shows that QB modification with acid (QB/Acid) and its magnetic nanocomposite (QB/MNPs) exhibited relatively more potential for Cr adsorption than several other adsorbents *e.g.*, Calcite based biocomposite (Mishra *et al.* 2020), Algal bloom/Iron-carbon composites (Cui *et al.* 2019), Chitosan carbonized rice husk (Sugashini and Begum 2013), food materials/Citric acid (Zhang *et al.* 2020), trimethyloctadecylammonium bromide impregnated on Artemisia monosperma (Ali HM *et al.* 2021) and activated carbon/micro-sized goethite composite (Su *et al.* 2019). The acid treated lantana camara (Nithya *et al.* 2020) showed higher Cr adsorption (362.8 mg/g) as compared with nanocomposite QB/MNPs used in the present study (Table 3).

4. Conclusions

The quinoa biosorbent (QB), its composite with magnetite nanoparticles (QB/MNPs) and acid activated QB (QB/Acid) were prepared and successfully applied for Cr (VI) removal from contaminated water. The FTIR analysis of pristine and Cr loaded adsorbents showed effective Cr loading onto the adsorbents surface. The Cr removal was greatly varied with the type of biosorbent, solution pH, Cr concentration, competing anions and contact time of adsorbent-adsorbate interaction. The optimum pH and dosage of the adsorbents (QB, QB/Acid and QB/MNPs) for highest Cr sequestration from water were pH 4, and 2 g/L, respectively. The maximum Cr removal was obtained in first 30 min due to saturation of the activated sites. The QB/MNPs showed highest Cr adsorption of 57.4 mg/L followed by QB/Acid (46.35 mg/g) and QB (39.9 mg/g). The presence of coexisting ions in water revealed a decline in the Cr removal from contaminated water. The experimental equilibrium isotherm data fitted well with Freundlich isotherm model while kinetic

isotherm data was well explained by pseudo-second order model. The reusability of QB/MNPs showed 5% reduction in Cr removal after five adsorption/desorption cycles. The obtained results proved that QB/MNPs composite is an inexpensive adsorbent with a higher reusability and adsorption potential for the sequestration of Cr from contaminated water.

Disclosure statement

The authors report there are no competing interests to declare.

Funding

Authors are grateful to Higher Education Commission (HEC) of Pakistan for financial support under NRPU with Project number [10377]. The authors extend their sincere appreciation to the Researchers Supporting Project number [RSP-2021/266] for the support, King Saud University, Riyadh, Saudi Arabia.

References

- Ahmad I, Akhtar MJ, Jadoon IBK, Imran M, Imran M, Ali S. 2017. Equilibrium modeling of cadmium biosorption from aqueous solution by compost. *Environ Sci Pollut Res Int.* 24(6):5277–5284. doi:10.1007/s11356-016-8280-y.
- Ahmad I, Farwa U, Khan ZUH, Imran M, Khalid MS, Zhu B, Rasool A, Shah GM, Tahir M, Ahmed M, et al. 2022. Biosorption and health risk assessment of arsenic contaminated water through cotton stalk biochar. *Surf Interfaces.* 29:101806.
- Aigbe UO, Das R, Ho WH, Srinivasu V, Maity A. 2018. A novel method for removal of Cr (VI) using polypyrrole magnetic nanocomposite in the presence of unsteady magnetic fields. *Sep Purif Technol.* 194:377–387. doi:10.1016/j.seppur.2017.11.057.
- Aigbe UO, Osibote OA. 2020. A review of hexavalent chromium removal from aqueous solutions by sorption technique using nanomaterials. *J Environ Chem Eng.* 8(6):104503. doi:10.1016/j.jece.2020.104503.
- Akram M, Khan B, Imran M, Ahmad I, Ajaz H, Tahir M, Rabbani F, Kaleem I, Nadeem Akhtar M, Ahmad N, et al. 2019. Biosorption of lead by cotton shells powder: characterization and equilibrium modeling study. *Int J Phytoremediation.* 21(2):138–144. doi:10.1080/15226514.2018.1488810.
- Ali A, Saeed K, Mabood F. 2016. Removal of chromium (VI) from aqueous medium using chemically modified banana peels as efficient low-cost adsorbent. *Alexandr Eng J.* 55(3):2933–2942. doi:10.1016/j.aej.2016.05.011.
- Ali HM, Essawy AA, Elnasr TAS, Aldawsari AM, Alshohaimi I, Hassan HM, Abdel-Farid IB. 2021. Selective and efficient sequestration of Cr (VI) in ground water using trimethyloctadecylammonium bromide impregnated on *Artemisia monosperma* plant powder. *J Taiwan Inst Chem Eng.* 125:122–131. doi:10.1016/j.jtice.2021.05.051.
- Aljerf L. 2018. High-efficiency extraction of bromocresol purple dye and heavy metals as chromium from industrial effluent by adsorption onto a modified surface of zeolite: kinetics and equilibrium study. *J Environ Manage.* 225:120–132. doi:10.1016/j.jenvman.2018.07.048.
- Basaldella EI, Vázquez PG, Iucolano F, Caputo D. 2007. Chromium removal from water using LTA zeolites: effect of pH. *J Colloid Interface Sci.* 313(2):574–578. doi:10.1016/j.jcis.2007.04.066.
- Bulgariu L, Ferțu DI, Cara IG, Gavrilăscu M. 2021. Efficacy of alkaline-treated soy waste biomass for the removal of heavy-metal ions and opportunities for their recovery. *Materials.* 14(23):7413. doi:10.3390/ma14237413.
- Cui Y, Masud A, Aich N, Atkinson JD. 2019. Phenol and Cr(VI) removal using materials derived from harmful algal bloom biomass: characterization and performance assessment for a biosorbent, a porous carbon, and Fe/C composites. *J Hazard Mater.* 368:477–486. doi:10.1016/j.jhazmat.2019.01.075.
- Deng Y, Tang L, Zeng G, Zhu Z, Yan M, Zhou Y, Wang J, Liu Y, Wang J. 2017. Insight into highly efficient simultaneous photocatalytic removal of Cr (VI) and 2, 4-dichlorophenol under visible light irradiation by phosphorus doped porous ultrathin g-C₃N₄ nanosheets from aqueous media: performance and reaction mechanism. *Appl Catal B Environ.* 203:343–354. doi:10.1016/j.apcatb.2016.10.046.
- Din SU, Khan MS, Hussain S, Imran M, Haq S, Hafeez M, Rehman FU, Chen X. 2021. Adsorptive mechanism of chromium adsorption on siltstone–nanomagnetite–biochar composite. *J Inorg Organomet Polym.* 31(4):1608–1620. doi:10.1007/s10904-020-01829-7.
- Din SU, Mahmood T, Naeem A, Shah NS, Hussain S, Imran M, Sultana S, Rehman AU. 2019. A novel insight into the adsorption interactions of arsenate with a Fe–Si binary oxide. *Colloid J.* 81(4):469–477. doi:10.1134/S1061933X19040045.
- Enniya I, Rghioui L, Jourani A. 2018. Adsorption of hexavalent chromium in aqueous solution on activated carbon prepared from apple peels. *Sustainable Chem Pharm.* 7:9–16. doi:10.1016/j.scp.2017.11.003.
- Estefan G, Sommer R, Ryan J. 2013. Methods of soil, plant, and water analysis. A manual for the West Asia and North Africa region 3: 65–119.
- Gorny J, Billon G, Noiriél C, Dumoulin D, Lesven L, Madé B. 2016. Chromium behavior in aquatic environments: a review. *Environ Rev.* 24(4):503–516. doi:10.1139/er-2016-0012.
- Guo H, Bi C, Zeng C, Ma W, Yan L, Li K, Wei K. 2018. *Camellia oleifera* seed shell carbon as an efficient renewable bio-adsorbent for the adsorption removal of hexavalent chromium and methylene blue from aqueous solution. *J Mol Liq.* 249:629–636. doi:10.1016/j.molliq.2017.11.096.
- Gupta VK, Rastogi A, Nayak A. 2010. Adsorption studies on the removal of hexavalent chromium from aqueous solution using a low cost fertilizer industry waste material. *J Colloid Interface Sci.* 342(1):135–141. doi:10.1016/j.jcis.2009.09.065.
- Hena S. 2010. Removal of chromium hexavalent ion from aqueous solutions using biopolymer chitosan coated with poly 3-methyl thiophene polymer. *J Hazard Mater.* 181(1–3):474–479. doi:10.1016/j.jhazmat.2010.05.037.
- Huang H, Wang Y, Zhang Y, Niu Z, Li X. 2020. Amino-functionalized graphene oxide for Cr (VI), Cu (II), Pb (II) and Cd (II) removal from industrial wastewater. *Open Chem.* 18(1):97–107. doi:10.1515/chem-2020-0009.
- Hussain M, Imran M, Abbas G, Shahid M, Iqbal M, Naeem MA, Murtaza B, Amjad M, Shah NS, Ul Haq Khan Z, et al. 2020. A new biochar from cotton stalks for As (V) removal from aqueous solutions: its improvement with H₃PO₄ and KOH. *Environ Geochem Health.* 42(8):2519–2534. doi:10.1007/s10653-019-00431-2.
- Imran M, Suddique M, Shah G, Ahmad I, Murtaza B, Shah N, Mubeen M, Ahmad S, Zakir A, Schotting R. 2019. Kinetic and equilibrium studies for cadmium biosorption from contaminated water using *Cassia fistula* biomass. *Int J Environ Sci Technol.* 16:3099–3108.
- Imran M, Anwar K, Akram M, Shah GM, Ahmad I, Samad Shah N, Khan ZUH, Rashid MI, Akhtar MN, Ahmad S, et al. 2019. Biosorption of Pb (II) from contaminated water onto *Moringa oleifera* biomass: kinetics and equilibrium studies. *Int J Phytoremediation.* 21(8):777–789. doi:10.1080/15226514.2019.1566880.
- Imran M, Iqbal MM, Iqbal J, Shah NS, Khan ZUH, Murtaza B, Amjad M, Ali S, Rizwan M. 2021. Synthesis, characterization and application of novel MnO and CuO impregnated biochar composites to sequester arsenic (As) from water: modeling, thermodynamics and reusability. *J Hazard Mater.* 401:123338. doi:10.1016/j.jhazmat.2020.123338.
- Imran M, Khan ZUH, Iqbal MM, Iqbal J, Shah NS, Munawar S, Ali S, Murtaza B, Naeem MA, Rizwan M. 2020. Effect of biochar modified with magnetite nanoparticles and HNO₃ for efficient removal of Cr

- (VI) from contaminated water: a batch and column scale study. *Environ Poll.* 261:114231. doi:10.1016/j.envpol.2020.114231.
- Iqbal J, Shah NS, Sayed M, Imran M, Muhammad N, Howari FM, Alkhoodri SA, Khan JA, Haq Khan ZU, Bhatnagar A, et al. 2019. Synergistic effects of activated carbon and nano-zerovalent copper on the performance of hydroxyapatite-alginate beads for the removal of As³⁺ from aqueous solution. *J Clean Prod.* 235:875–886. doi:10.1016/j.jclepro.2019.06.316.
- Iqbal MM, Imran M, Hussain T, Naeem MA, Al-Kahtani AA, Shah GM, Ahmad S, Farooq A, Rizwan M, Majeed A, et al. 2021. Effective sequestration of Congo red dye with ZnO/cotton stalks biochar nanocomposite: modeling, reusability and stability. *J Saudi Chem Soc.* 25(2):101176. doi:10.1016/j.jscs.2020.101176.
- Jarvis DE, Ho YS, Lightfoot DJ, Schmöckel SM, Li B, Borm TJA, Ohyanagi H, Mineta K, Michell CT, Saber N, et al. 2017. The genome of *Chenopodium quinoa*. *Nature.* 542(7641):307–312. doi:10.1038/nature21370.
- Khan ZUH, Khan A, Shah NS, Din IU, Salam MA, Iqbal J, Muhammad N, Imran M, Ali M, Sayed M, et al. 2021. Photocatalytic and biomedical investigation of green synthesized NiONPs: toxicities and degradation pathways of Congo red dye. *Surf Interfaces.* 23:100944. doi:10.1016/j.surfin.2021.100944.
- Khan ZUH, Sadiq HM, Shah NS, Khan AU, Muhammad N, Hassan SU, Tahir K, Safi SZ, Khan FU, Imran M, et al. 2019. Greener synthesis of zinc oxide nanoparticles using *Trianthema portulacastrum* extract and evaluation of its photocatalytic and biological applications. *J Photochem Photobiol B.* 192:147–157. doi:10.1016/j.jphoto.2019.01.013.
- Khalifa EB, Rzig B, Chakroun R, Nouagui H, Hamrouni B. 2019. Application of response surface methodology for chromium removal by adsorption on low-cost biosorbent. *Chemom Intell Lab Syst.* 189:18–26. doi:10.1016/j.chemolab.2019.03.014.
- Kumar A, Thakur A, Panesar PS. 2019. Extraction of hexavalent chromium by environmentally benign green emulsion liquid membrane using tridodecylamine as an extractant. *J Ind Eng Chem.* 70:394–401. doi:10.1016/j.jiec.2018.11.002.
- Kumar S, Narayanasamy S, Venkatesh RP. 2019. Removal of Cr (VI) from synthetic solutions using water caltrop shell as a low-cost biosorbent. *Sep Sci Technol.* 54(17):2783–2799. doi:10.1080/01496395.2018.1560333.
- Kumar A, Patra C, Kumar S, Narayanasamy S. 2022. Effect of magnetization on the adsorptive removal of an emerging contaminant ciprofloxacin by magnetic acid activated carbon. *Environ Res.* 206:112604. doi:10.1016/j.envres.2021.112604.
- Li K, Li P, Cai J, Xiao S, Yang H, Li A. 2016. Efficient adsorption of both methyl orange and chromium from their aqueous mixtures using a quaternary ammonium salt modified chitosan magnetic composite adsorbent. *Chemosphere.* 154:310–318. doi:10.1016/j.chemosphere.2016.03.100.
- Liu F, Yu J, Tu G, Qu L, Xiao J, Liu Y, Wang L, Lei J, Zhang J. 2017. Carbon nitride coupled Ti-SBA15 catalyst for visible-light-driven photocatalytic reduction of Cr (VI) and the synergistic oxidation of phenol. *Appl Catal B Environ.* 201:1–11. doi:10.1016/j.apcatb.2016.08.001.
- Liu W, Ni J, Yin X. 2014. Synergy of photocatalysis and adsorption for simultaneous removal of Cr (VI) and Cr (III) with TiO₂ and titanate nanotubes. *Water Res.* 53:12–25. doi:10.1016/j.watres.2013.12.043.
- Lucaci A-R, Bulgariu D, Bulgariu L. 2021. In situ functionalization of iron oxide particles with alginate: a promising biosorbent for retention of metal ions. *Polymers.* 13(20):3554. doi:10.3390/polym13203554.
- Lyu H, Tang J, Huang Y, Gai L, Zeng EY, Liber K, Gong Y. 2017. Removal of hexavalent chromium from aqueous solutions by a novel biochar supported nanoscale iron sulfide composite. *Chem Eng J.* 322:516–524. doi:10.1016/j.cej.2017.04.058.
- Ma H, Yang J, Gao X, Liu Z, Liu X, Xu Z. 2019. Removal of chromium (VI) from water by porous carbon derived from corn straw: influencing factors, regeneration and mechanism. *J Hazard Mater.* 369:550–560. doi:10.1016/j.jhazmat.2019.02.063.
- Maitlo HA, Kim K-H, Kumar V, Kim S, Park J-W. 2019. Nanomaterials-based treatment options for chromium in aqueous environments. *Environ Int.* 130:104748.
- Mishra A, Gupta B, Kumar N, Singh R, Varma A, Thakur IS. 2020. Synthesis of calcite-based bio-composite biochar for enhanced bio-sorption and detoxification of chromium Cr (VI) by *Zhihengliuella* sp. *ISTPL4. Bioresour Technol.* 307:123262. doi:10.1016/j.biortech.2020.123262.
- Mor S, Ravindra K, Bishnoi N. 2007. Adsorption of chromium from aqueous solution by activated alumina and activated charcoal. *Bioresour Technol.* 98(4):954–957. doi:10.1016/j.biortech.2006.03.018.
- Murtaza B, Shah NS, Sayed M, Khan JA, Imran M, Shahid M, Khan ZUH, Ghani A, Murtaza G, Muhammad N, et al. 2019. Synergistic effects of bismuth coupling on the reactivity and reusability of zero-valent iron nanoparticles for the removal of cadmium from aqueous solution. *Sci Total Environ.* 669:333–341. doi:10.1016/j.scitotenv.2019.03.062.
- Naeem MA, Imran M, Amjad M, Abbas G, Tahir M, Murtaza B, Zakir A, Shahid M, Bulgariu L, Ahmad I. 2019. Batch and column scale removal of cadmium from water using raw and acid activated wheat straw biochar. *Water.* 11(7):1438. doi:10.3390/w11071438.
- Naeem MA, Shabbir A, Amjad M, Abbas G, Imran M, Murtaza B, Tahir M, Ahmad A. 2020. Acid treated biochar enhances cadmium tolerance by restricting its uptake and improving physio-chemical attributes in quinoa (*Chenopodium quinoa* Willd.). *Ecotoxicol Environ Saf.* 191:110218. doi:10.1016/j.ecoenv.2020.110218.
- Naushad M, ALOthman Z, Awual M, Alam MM, Eldesoky G. 2015. Adsorption kinetics, isotherms, and thermodynamic studies for the adsorption of Pb²⁺ and Hg²⁺ metal ions from aqueous medium using Ti (IV) iodovanadate cation exchanger. *Ionics.* 21(8):2237–2245. doi:10.1007/s11581-015-1401-7.
- Nithya K, Sathish A, Kumar PS. 2020. Packed bed column optimization and modeling studies for removal of chromium ions using chemically modified *Lantana camara* adsorbent. *J Water Process Eng.* 33:101069. doi:10.1016/j.jwpe.2019.101069.
- Ogata F, Nagai N, Itami R, Nakamura T, Kawasaki N. 2020. Potential of virgin and calcined wheat bran biomass for the removal of chromium (VI) ion from a synthetic aqueous solution. *J Environ Chem Eng.* 8(2):103710. doi:10.1016/j.jece.2020.103710.
- Ou J-H, Sheu Y-T, Tsang DCW, Sun Y-J, Kao C-M. 2020. Application of iron/aluminum bimetallic nanoparticle system for chromium-contaminated groundwater remediation. *Chemosphere.* 256:127158. doi:10.1016/j.chemosphere.2020.127158.
- Patra C, Mediseti RMN, Pakshirajan K, Narayanasamy S. 2019. Assessment of raw, acid-modified and chelated biomass for sequestration of hexavalent chromium from aqueous solution using *Sterculia villosa* Roxb. shells. *Environ Sci Pollut Res Int.* 26(23):23625–23637. doi:10.1007/s11356-019-05582-4.
- Patra C, Shahnaz T, Subbiah S, Narayanasamy S. 2020. Comparative assessment of raw and acid-activated preparations of novel *Pongamia pinnata* shells for adsorption of hexavalent chromium from simulated wastewater. *Environ Sci Pollut Res Int.* 27(13):14836–14851. doi:10.1007/s11356-020-07979-y.
- Pradhan D, Sukla LB, Mishra BB, Devi N. 2019. Biosorption for removal of hexavalent chromium using microalgae *Scenedesmus* sp. *J Clean Prod.* 209:617–629. doi:10.1016/j.jclepro.2018.10.288.
- Ruiz K, Biondi S, Martínez E, Orsini F, Antognoni F, Jacobsen S-E. 2016. Quinoa—a model crop for understanding salt-tolerance mechanisms in halophytes. *Plant Biosyst.* 150(2):357–371. doi:10.1080/11263504.2015.1027317.
- Shabbir A, Saqib M, Murtaza G, Abbas G, Imran M, Rizwan M, Naeem MA, Ali S, Javeed HMR. 2021. Biochar mitigates arsenic-induced human health risks and phytotoxicity in quinoa under saline conditions by modulating ionic and oxidative stress responses. *Environ Pollut.* 287:117348. doi:10.1016/j.envpol.2021.117348.
- Shah G, Imran M, Bakhat H, Hammad H, Ahmad I, Rabbani F, Khan Z. 2019. Kinetics and equilibrium study of lead bio-sorption from contaminated water by compost and biogas residues. *Int J Environ Sci Technol.* 16(7):3839–3850. doi:10.1007/s13762-018-1865-x.

- Shah NS, Khan JA, Sayed M, Khan ZUH, Iqbal J, Imran M, Murtaza B, Zakir A, Polychronopoulou K. 2020. Nano zerovalent zinc catalyzed peroxymonosulfate based advanced oxidation technologies for treatment of chlorpyrifos in aqueous solution: a semi-pilot scale study. *J Clean Prod.* 246:119032. doi:10.1016/j.jclepro.2019.119032.
- Shah GM, Imran M, Aiman U, Iqbal MM, Akram M, Javeed HMR, Waqar A, Rabbani F. 2022. Efficient sequestration of lead from aqueous systems by peanut shells and compost: evidence from fixed bed column and batch scale studies. *PeerJ Physical Chemistry.* 4, e21.
- Shafiq M, Alazba A, Amin M. 2018. Removal of heavy metals from wastewater using date palm as a biosorbent: a comparative review. *JSM.* 47(1):35–49. doi:10.17576/jsm-2018-4701-05.
- Shakya A, Agarwal T. 2019. Removal of Cr (VI) from water using pineapple peel derived biochars: adsorption potential and re-usability assessment. *J Mol Liq.* 293:111497. doi:10.1016/j.molliq.2019.111497.
- Shamsollahi Z, Partovinia A. 2019. Recent advances on pollutants removal by rice husk as a bio-based adsorbent: a critical review. *J Environ Manage.* 246:314–323. doi:10.1016/j.jenvman.2019.05.145.
- Sharma M, Joshi M, Nigam S, Shree S, Avasthi DK, Adelong R, Srivastava SK, Mishra YK. 2019. ZnO tetrapods and activated carbon based hybrid composite: adsorbents for enhanced decontamination of hexavalent chromium from aqueous solution. *Chem Eng J.* 358:540–551. doi:10.1016/j.cej.2018.10.031.
- Sharma PK, Ayub S, Tripathi CN. 2016. Isotherms describing physical adsorption of Cr (VI) from aqueous solution using various agricultural wastes as adsorbents. *Cogent Eng.* 3(1):1186857. doi:10.1080/23311916.2016.1186857.
- Sharma G, Naushad M. 2020. Adsorptive removal of noxious cadmium ions from aqueous medium using activated carbon/zirconium oxide composite: isotherm and kinetic modelling. *J Mol Liq.* 310:113025. doi:10.1016/j.molliq.2020.113025.
- Su M, Fang Y, Li B, Yin W, Gu J, Liang H, Li P, Wu J. 2019. Enhanced hexavalent chromium removal by activated carbon modified with micro-sized goethite using a facile impregnation method. *Sci Total Environ.* 647:47–56. doi:10.1016/j.scitotenv.2018.07.372.
- Suganya E, Saranya N, Sivaprakasam S, Varghese LA, Narayanasamy S. 2020. Experimentation on raw and phosphoric acid activated *Eucalyptus camadulensis* seeds as novel biosorbents for hexavalent chromium removal from simulated and electroplating effluents. *Environ Technol Innov.* 19:100977. doi:10.1016/j.eti.2020.100977.
- Sugashini S, Begum KMS. 2013. Optimization using central composite design (CCD) for the biosorption of Cr (VI) ions by cross linked chitosan carbonized rice husk (CCACR). *Clean Techn Environ Policy.* 15(2):293–302. doi:10.1007/s10098-012-0512-3.
- Tariq MA, Nadeem M, Iqbal MM, Imran M, Siddique MH, Iqbal Z, Amjad M, Rizwan M, Ali S. 2020. Effective sequestration of Cr (VI) from wastewater using nanocomposite of ZnO with cotton stalks biochar: modeling, kinetics, and reusability. *Environ Sci Pollut Res Int.* 27(27):33821–33834. doi:10.1007/s11356-020-09481-x.
- Vigneshwaran S, Sirajudheen P, Karthikeyan P, Meenakshi S. 2021. Fabrication of sulfur-doped biochar derived from tapioca peel waste with superior adsorption performance for the removal of Malachite green and Rhodamine B dyes. *Surf Interfaces.* 23:100920. doi:10.1016/j.surf.2020.100920.
- Vilela PB, Dalalibera A, Duminelli EC, Becegato VA, Paulino AT. 2019. Adsorption and removal of chromium (VI) contained in aqueous solutions using a chitosan-based hydrogel. *Environ Sci Pollut Res.* 26(28):28481–28489. doi:10.1007/s11356-018-3208-3.
- Wang C-C, Du X-D, Li J, Guo X-X, Wang P, Zhang JJ. 2016. Photocatalytic Cr (VI) reduction in metal-organic frameworks: a mini-review. *Appl Catal B Environ.* 193:198–216. doi:10.1016/j.apcatb.2016.04.030.
- Wang H, Zhang M, Li H. 2019. Synthesis of nanoscale zerovalent iron (nZVI) supported on biochar for chromium remediation from aqueous solution and soil. *IJERPH.* 16(22):4430. doi:10.3390/ijerph16224430.
- Xie W, Zhang M, Liu D, Lei W, Sun L, Wang X. 2017. Photocatalytic TiO₂/porous BNNs composites for simultaneous LR2B and Cr (VI) removal in wool dyeing bath. *J Photochem Photobiol A Chem.* 333: 165–173. doi:10.1016/j.jphotochem.2016.10.024.
- Yi G, Xing B, Zeng H, Wang X, Zhang C, Cao J, Chen L. 2017. One-step synthesis of hierarchical micro-mesoporous SiO₂/reduced graphene oxide nanocomposites for adsorption of aqueous Cr (VI). *J Nanomater.* 2017:1–10. doi:10.1155/2017/6286549.
- Yi Y, Lv J, Liu Y, Wu G. 2017. Synthesis and application of modified litchi peel for removal of hexavalent chromium from aqueous solutions. *J Mol Liq.* 225:28–33. doi:10.1016/j.molliq.2016.10.140.
- Zeng H, Zeng H, Zhang H, Shahab A, Zhang K, Lu Y, Nabi I, Naseem F, Ullah H. 2021. Efficient adsorption of Cr (VI) from aqueous environments by phosphoric acid activated eucalyptus biochar. *J Clean Prod.* 286:124964.
- Zhang D, Xu W, Cai J, Cheng S-Y, Ding W-P. 2020. Citric acid-incorporated cellulose nanofibrous mats as food materials-based biosorbent for removal of hexavalent chromium from aqueous solutions. *Int J Biol Macromol.* 149:459–466. doi:10.1016/j.ijbiomac.2020.01.199.
- Zhao R, Li X, Li Y, Li Y, Sun B, Zhang N, Chao S, Wang C. 2017. Functionalized magnetic iron oxide/polyacrylonitrile composite electrospun fibers as effective chromium (VI) adsorbents for water purification. *J Colloid Interface Sci.* 505:1018–1030. doi:10.1016/j.jcis.2017.06.094.
- Zhu K, Duan Y, Wang F, Gao P, Jia H, Ma C, Wang C. 2017. Silane-modified halloysite/Fe₃O₄ nanocomposites: simultaneous removal of Cr (VI) and Sb (V) and positive effects of Cr (VI) on Sb (V) adsorption. *Chem Eng J.* 311:236–246. doi:10.1016/j.cej.2016.11.101.